

Intramolecular Donor Strand Complementation in the *E. coli* Type 1 Pilus Subunit FimA Explains the Existence of FimA Monomers As Off-Pathway Products of Pilus Assembly That Inhibit Host Cell Apoptosis

Michal J. Walczak, Chasper Puorger, Rudi Glockshuber and Gerhard Wider

ETH Zurich Institute of Molecular Biology and Biophysics, CH-8093 Zurich, Switzerland

Correspondence to Rudi Glockshuber and Gerhard Wider: rudi@mol.biol.ethz.ch; gsw@mol.biol.ethz.ch
<http://dx.doi.org/10.1016/j.jmb.2013.10.029>

Edited by I. Shimada

Abstract

Type 1 pili are filamentous organelles mediating the attachment of uropathogenic *Escherichia coli* to epithelial cells of host organisms. The helical pilus rod consists of up to 3000 copies of the main structural subunit FimA that interact via donor strand complementation, where the incomplete Ig-like fold of FimA is completed by insertion of the N-terminal extension (donor strand) of the following FimA subunit. Recently, it was shown that FimA also exists in a monomeric, assembly-incompetent form and that FimA monomers act as inhibitors of apoptosis in infected host cells. Here we present the NMR structure of monomeric wild-type FimA with its natural N-terminal donor strand complementing the Ig fold. Compared to FimA subunits in the assembled pilus, intramolecular self-complementation in the monomer stabilizes the FimA fold with significantly less interactions, and the natural FimA donor strand is inserted in the opposite orientation. In addition, we show that a motif of two glycine residues in the FimA donor strand, separated by five residues, is the prerequisite of the alternative, parallel donor strand insertion mechanism in the FimA monomer and that this motif is preserved in FimA homologs of many enteroinvasive pathogens. We conclude that FimA is a unique case of a protein with alternative, functionally relevant folding possibilities, with the FimA polymer forming the highly stable pilus rod and the FimA monomer promoting pathogen propagation by apoptosis suppression of infected epithelial target cells.

© 2013 Elsevier Ltd. All rights reserved.

Introduction

Type 1 pili are thread-like structures on the surface of uropathogenic *Escherichia coli* strains, which are essential for bacterial attachment to epithelial cells of the urinary tract. The pili consist of a short fibrillar tip structure and a rod-shaped main structure that is attached to the bacterial outer membrane via the pilus assembly platform FimD. The fibrillar tip consists of the protein subunits FimF and FimG and the adhesin FimH that recognizes mannose units in the glycoprotein receptor Uroplakin Ia [1,2]. The pilus rod is composed of up to 3000 copies of the main subunit FimA, which assemble into a right-handed, helical quaternary structure. Type 1 pili are assembled *in vivo* via the chaperone/usher pathway [3,4]. All structural subunits are homologous proteins sharing an immu-

noglobulin (Ig)-like fold. After secretion of the subunits into the periplasm, their single and invariant disulfide bond is formed by disulfide exchange with the dithiol oxidase DsbA [5]. Folding of the disulfide-intact subunits is subsequently catalyzed by the pilus assembly chaperone FimC [5,6] that stays bound to the native subunits and delivers them to the outer membrane assembly platform (usher) FimD where the subunits are incorporated into the growing pilus [7–9]. Neighboring subunits in the pilus interact via a mechanism termed donor strand complementation [10] in which the incomplete Ig-like fold of each subunit [lacking the seventh (last) β -strand of the Ig fold] is completed by an N-terminal extension (donor strand) of the following subunit that inserts in an antiparallel orientation relative to the sixth strand [10,11]. In FimC–subunit complexes, the lacking strand is

provided to the subunit by an extended segment (donor strand) of FimC that, however, inserts in a parallel orientation relative to the subunit's C-terminal (F) strand [10,12,13]. During subunit incorporation into the growing pilus, the donor strand of the chaperone is displaced by an N-terminal donor strand extension of the next, incoming subunit [14,15].

Besides the “antiparallel” orientation of the donor strand, subunit–subunit contacts are characterized by an almost perfect surface complementarity between the subunit and bound donor strand and an infinite stability against dissociation [13,16–18]. In contrast, the interactions between the FimC donor strand and FimC-bound subunits are less extensive, keeping the subunits in a less compact, assembly-competent state that allows dissociation from the chaperone during pilus assembly [19].

In a previous study, we have determined the NMR structure of FimAa, a self-complemented variant of FimA that is extended at the C-terminus by a hexaglycine linker followed by a second copy of the FimA donor strand [residues 1–20 in wild-type (wt) FimA] (Fig. 1) [12]. The structure showed that

FimAa incorporated the C-terminal copy of the donor strand sequence into its fold in exactly the same manner (antiparallel donor strand insertion) as that observed in the quaternary structure of the pilus (Fig. 1). In addition, we showed that FimAa is extremely stable against unfolding, with a free energy of folding of -85 kJ/mol. Moreover, we obtained clear evidence that FimA wt is capable of intramolecular self-complementation by insertion of its natural, N-terminal donor strand into the FimA fold, a property that has not been observed so far for any other type 1 pilus subunit [6,20]. In contrast to FimAa, self-complemented FimA wt proved to be a monomer that is however less stable against unfolding than FimAa ($\Delta G_{\text{fold}}^0 = -10$ kJ/mol) (Fig. 1). We speculated that the FimA monomer is generated by insertion of the natural FimA donor of FimA into its own pilin domain in a “parallel” orientation because a FimA variant depleted of the donor strand proved folding incompetent [12]. The results showed that FimAa with its duplication of the donor strand segment at its N-terminus and C-terminus is a unique case of a protein with alternative folding possibilities and spontaneously adopts the thermodynamically

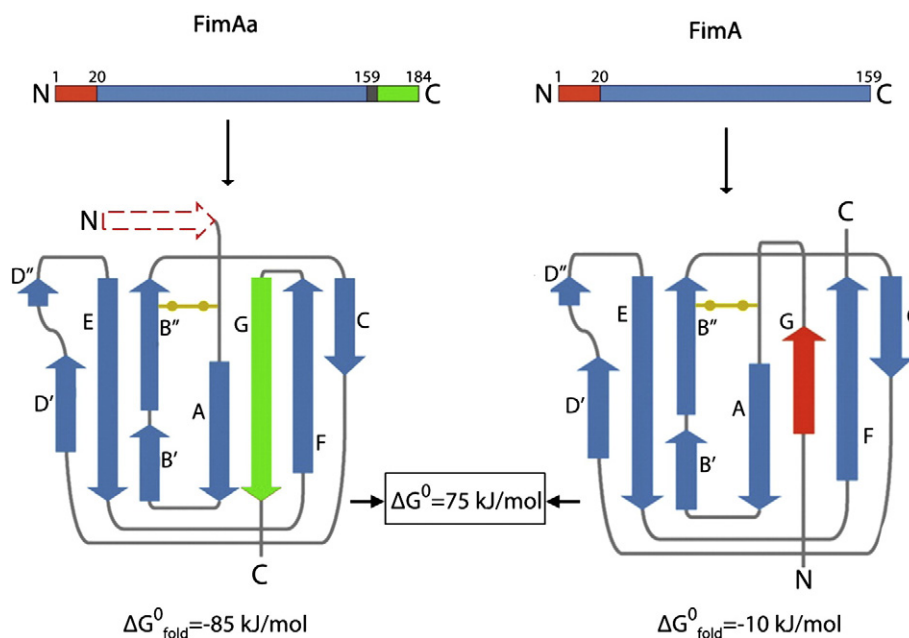


Fig. 1. Folding scheme and thermodynamic stability of the self-complemented variant FimAa (left) and FimA wt (right) as determined previously [12]. Top left: FimAa is composed of an N-terminal donor strand extension (residues 1–20; red) and a larger part (residues 21–159; blue) forming an incomplete Ig-like fold; the natural FimA sequence (shown on top right) is extended at the C-terminus by a hexaglycine linker (G6, gray) and a second copy of the donor strand segment (green). Bottom: FimAa is a protein with alternative folding possibilities that spontaneously adopts the most stable conformation, characterized by the insertion of the C-terminal copy of the donor strand into the FimA pilin fold in an antiparallel orientation relative to the C-terminal F-strand completing the Ig-like fold (left β -sheet topology diagram). Here we confirm the previous hypothesis [12] that FimA wt is also capable of intramolecular self-complementation through insertion of its natural, N-terminal donor strand in a parallel orientation relative to the F-strand (right β -sheet topology diagram). The conformation with the C-terminal donor strand insertion was shown to be 75 kJ/mol more stable than that with the N-terminal donor strand insertion adopted by FimA wt [12]. The red broken arrow represents the flexibly disordered donor strand segment that is not incorporated into the tertiary structure of FimAa. The single, invariant disulfide bond of FimA is indicated in yellow.

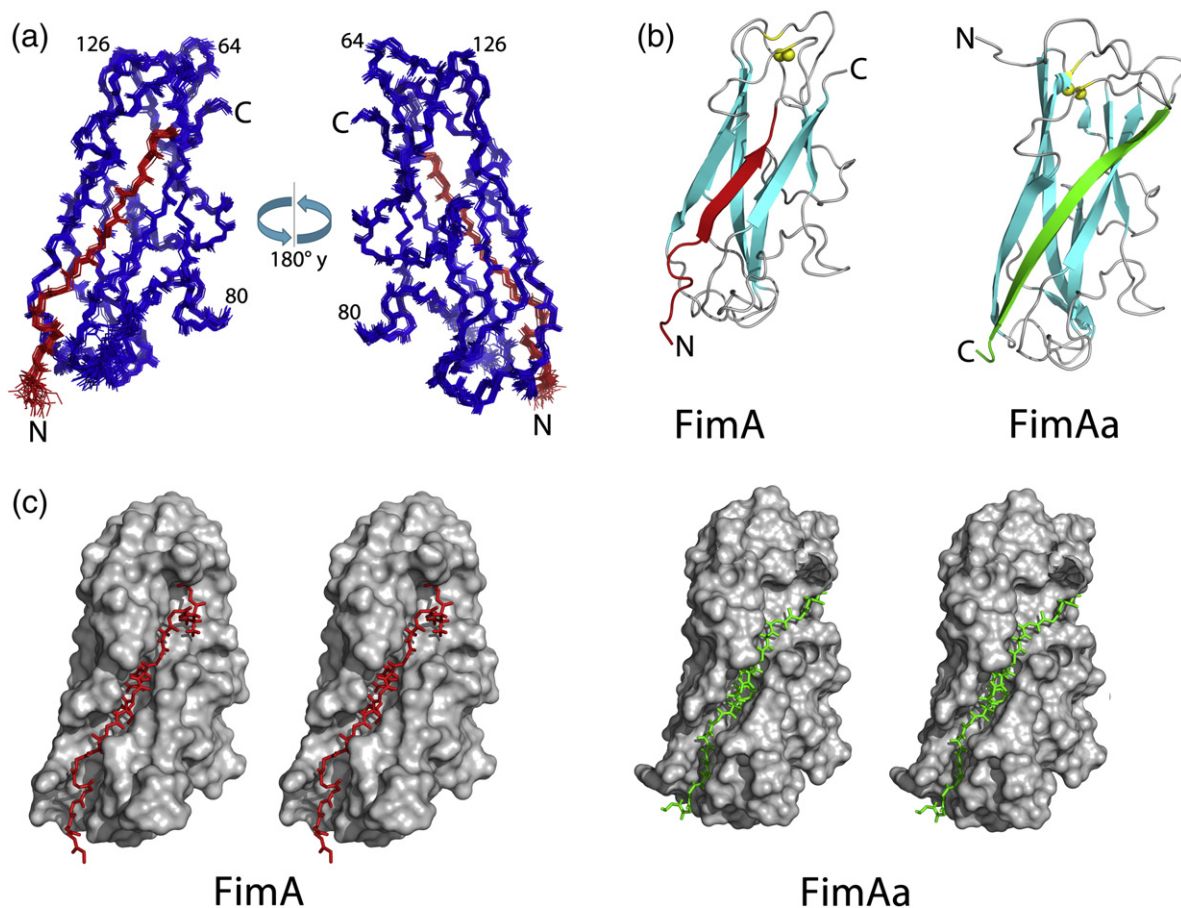


Fig. 2. NMR structure of FimA wt. (a) View of the protein backbone represented by the 20 conformers with the lowest energy. The N-terminal part in FimA that self-complements the β -sheet fold is shown in red; numbers indicate sequence positions. (b) Cartoon drawing of FimA and FimAa conformers with the best target function: the donor strand segments complementing the FimA pilin fold are shown in red and green for FimA and FimAa, respectively; the side chains of the cysteine pair forming the single disulfide bond in FimA are indicated in yellow, and the sulfur atoms are shown as yellow spheres. (c) Stereo view of a surface representation of FimA wt and FimAa. The complementing β -strands inserted in the binding groove are presented as a stick model in red (FimA) and green (FimAa). Figures (a), (b) and (c) were prepared with PyMOL [22]. FimA wt was expressed and purified as described previously [12]. Uniformly ^{13}C , ^{15}N -labeled FimA was expressed in *E. coli* BL21 (DE3) strains in minimal M9 medium containing $^{15}\text{NH}_4\text{Cl}$ (1 g/l) and ^{13}C -labeled glucose (3 g/l) as only nitrogen and carbon sources, respectively. The concentration of FimA wt (1.2 mM) was determined by NMR with the PULCON method [23]. NMR data were collected at 25 °C in 20 mM sodium phosphate (pH 7.0) on a Bruker 750-MHz and 900-MHz spectrometer. Spectra processing was performed with Topspin 2.1 (Bruker, Karlsruhe, Germany) and analyzed with CARA (cara.nmr.ch). Backbone resonance assignment was achieved based on [^{15}N , ^1H]HSQC (heteronuclear single quantum coherence), [^{13}C , ^1H]HSQC, HNCA, HN(CO)CA and HNCACB experiments [24]. Side-chain resonance assignment was obtained using HCCH-TOCSY (total correlated spectroscopy), HCCH-COSY and ^{15}N - and ^{13}C -resolved [^1H , ^1H]NOESY (NOE spectroscopy) experiments [24]. Assignment of aromatic residues was performed with two-dimensional CBHD, ct-[^{13}C , ^1H]HSQC and ^{13}C -resolved [^1H , ^1H]NOESY experiments [24]. The structure calculation was carried out with ATNOS/CANDID [25,26] and CYANA 3.0 [27]. The amino acid sequence, the chemical shift list and the three-dimensional NOESY spectra were used as input supplemented by restraints for the disulfide bond between Cys21 and Cys61. The structure calculation followed the standard protocol with seven cycles. Energy minimization was performed with CNS in a water shell [28]. The 20 lowest-energy conformers were analyzed with PyMOL [22] and PROCHECK [29]. The coordinates of the ensemble of 20 conformers of FimA have been deposited in the Protein Data Bank with the entry code 2M5G.

more stable conformation in solution (Fig. 1). Here we present the NMR structure of FimA wt. The results demonstrate that the donor strand indeed complements the fold of FimA in *cis* by parallel insertion relative to the C-terminal F-strand and show the exact

register of donor strand insertion, providing the structural basis for the existence of stable, soluble FimA monomers that have been reported recently to suppress host cell apoptosis as a response to type 1 pilus-mediated pathogen internalization [21].

Table 1. Input for the structure calculation and characterization of the energy-minimized NMR structure of FimA.

Quantity	Value ^a
NOE upper distance limits	3530
Residual target function (Å ²)	1.01 ± 0.017
Residual NOE violations	
Number ≥ 0.2 Å	3
Maximum (Å)	0.0217
Residual angle violations	
Number ≥ 2.5°	0
Maximum (°)	0.255
Hydrogen bonds	47
r.m.s.d. to the mean coordinates for residues 2–158 (Å)	
N, C ^α , C' (backbone)	0.40 ± 0.04
All heavy atoms	0.60 ± 0.04
Ramachandran plot statistics ^b (%)	
Most favored regions	81.5
Additional allowed regions	18.3
Generously allowed regions	0.2
Disallowed regions	0.0

NOE, nuclear Overhauser enhancement.

^a Except for the first top entry, the average value for 20 energy-minimized conformers with the lowest residual ATNOS/CANDID [25,26] target function values and standard deviation among them are given.

^b As determined by PROCHECK [29].

NMR structure of FimA

Our previous studies on FimA wt showed that the protein forms a well-soluble monomer with intact tertiary structure in the absence of the assembly chaperone FimC or partner subunits [12]. This was confirmed by its well-resolved amide group correlation spectrum (see Fig. S1). Figure 2 shows the solved NMR structure of FimA wt (residues 1–159). The structure could be determined with high precision [r.m.s.d. values for the 20 conformers representing the NMR structure are 0.58 Å and 0.88 Å for the backbone and heavy atoms, respectively (Table 1)]. FimA wt indeed inserts its N-terminal extension (residues 1–20) into its fold but, otherwise, adopts the same β-sheet topology for residues 21–159 as the one observed for FimAa [12] and other pilus subunits from chaperone–usher systems [10,13,30–32]. In contrast to all other structures of pilin domains in the absence of an assembly chaperone, the natural N-terminal extension of FimA wt [G-strand in the solved NMR structure (Fig. 1b)] complements the Ig fold in a non-canonical manner; that is, it is oriented parallel with the F-strand. As observed for FimAa, the fold of FimA is mainly determined by two β-sheets, the first being composed of strand A (28–37), the donor strand G (8–13), strand F (148–155) and strand

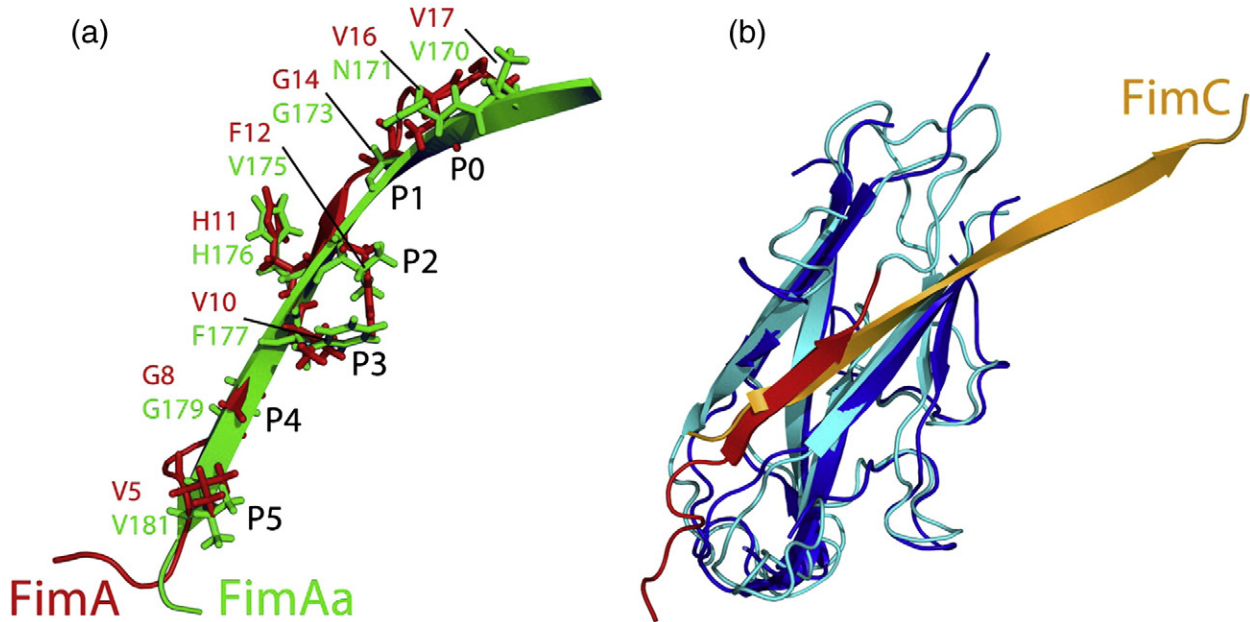
C (69–74) and the second being composed of strands B' (45–48), B'' (51–57), E (127–137), D' (98–102) and D'' (122–123). The two β-sheets are packed against each other in a wound fashion (Fig. 1b). In addition, a one-turn α-helix (residues 24–28) and two one-turn ₃₁₀ helices (40–42 and 79–83) could be identified. Except for residues 1–20, the structure and the secondary structure boundaries [33] are almost identical with those in the NMR structure of FimAa [12].

Intermolecular donor strand complementation between neighboring pilus subunits is characterized by the presence of five specific side-chain binding pockets in the pilin domain, termed P1–P5, in addition to the intermolecular β-sheet hydrogen bonds formed by main-chain atoms [34]. Figure 3a shows that the pockets P1–P3 in the FimA donor strand binding groove are occupied by the donor strand residues Val16 (P1), Phe12 (P2) and Val10 (P3). The FimA residue Gly8 occupies the same cavity (P4) as Gly179 of FimAa (Fig. 3a). The P4 pocket is very shallow due to the presence of the bulky side chain of Tyr137 and sterically can only accommodate a Gly residue without disrupting the main-chain β-sheet hydrogen bond network between donor strand and pilin domain (Fig. 3). Gly8 at P4 thus defines the register of the parallel donor strand insertion. Notably, the P5 pocket is occupied by Val5 in FimA wt (corresponding to Val181 in FimAa). While every second side chain of the FimAa donor strand from position 173 to position 181 is inserted into P1–P5, this pattern is disrupted with the insertion of Val5 into the P5 pocket in FimA. In general, bulky side chains of phenylalanines and valines adopt the same orientations in both FimA wt and FimAa, inserting deeply into their corresponding pockets. In the P1 pocket, the side chains of Val16 (FimA wt) and Asn171 (FimAa) are not positioned identically; however, both orientations are sterically possible.

In addition to the NMR structures of FimA and FimAa, a crystal structure of the variant FimA_t in complex with FimC has been solved [5]. FimA_t is a FimA variant lacking the N-terminal 17 residues to prevent formation of FimA homopolymers. A comparison of the structures of FimA wt and FimA_t (PDB ID: 4DWH) reveals close similarity of the overall folds of the proteins (Fig. 3b). Small differences are observed in the lengths of some β-strands and their exact positioning in the sequence. For example, using the letter code of Fig. 1, β-strand A spreads from residue D29 to residue G35 in FimA and from T30 to Q33 in FimA_t. The short strand B' (E45 to T48 in FimA_t) is poorly defined in the NMR ensemble of FimA. The β-strand D' extends from V99 to L104 in FimA, whereas in FimA_t it starts at T97. In FimA wt, strand D' is followed by residual strand D'' that is not present in the X-ray structure of FimA_t. The

subsequent β -strand, E, is substantially longer in the FimA_t (T130-T144) than in FimA (N129-A139). The only outstanding difference between FimA wt and FimA_t in complex with FimC is the length of the

inserted donor strand G, which is short in FimA wt (G8-K13) and long in FimA_t (T102-R116) (Fig. 3b). This can be explained by the fact that strand G, which is donated to FimA_t by FimC in the FimA_t-



(c)

FimA

1 AATTVNGGT¹⁰VHFKGEVVNA¹⁹

FimAa

184 ANVVEGKFHVT¹⁷⁵GGNVTTAA¹⁶⁵

(d)

Uropathogenic *E. coli* FimA

-----ATTVNGGTVHFKGEVVNAA

Shigella flexneri FimA

SSAAALADTTTVNGGTIHFKGEVVNAA

Klebsiella pneumoniae FimA

SSAAALADTTTVNGGTVHFKGEVVNAA

Salmonella gallinarum FimA

AAVAADPTPVSVSGGTIHFEKGLVNAA

Salmonella enterica FimA

-----PTPVSVSGGTIHFEKGLVNAA

Escherichia coli PapA

-----AAPTIPQGQGEVTFKGTVVDAP

Aeromonas salmonicida FimA

LLCGSAVAAGGAGSGKVTFNGEIINAP

Burkholderia mallei FimA

ACAALSTSAFAAGTGTLNFTGEIVAGA

Bordetella parapertussis FimA

T----YQHQVFAADGTLVITGAITDIT

Chromobacterium violaceum FimA

IGLGVYSSGAMAADGKITVTGNIVAQT

Serratia marcescens FimA

LVLSATASNAMAANGTVKFTGEIKQST

Alcanivorax borkumensis FimA

AAISGISSIAIANTGEVIFNGVVSDDT

Porphyromonas gingivalis FimACSAGQRTLVMANTGAMELV¹⁷⁵GKTLAEV

FimC complex, not only complements the β -sheet of FimA_t but also extends into FimC where it contributes a strand to the β -sheet of FimC, that is, the structures share a β -strand.

Discussion

FimA wt has a strongly reduced thermodynamic stability compared to FimAa that mimics the intermolecular donor strand complementation between neighboring FimA subunits in the assembled type 1 pilus rod [12]. The interrupted and shorter, parallel β -sheet architecture formed by the strands G and F in FimA wt is the most obvious structural explanation for the dramatically decreased stability (70 kJ/mol) of FimA wt relative to FimAa. Despite their different stabilities, FimA wt and FimAa show identical and very low rates of spontaneous folding (about 1.6 h half-life) [5,12]. Their stability difference is thus exclusively caused by a 13 orders of magnitude lower unfolding rate of FimAa [12]. As FimA folding is strictly dependent on donor strand insertion into the FimA fold [12], these observations, together with the present structure, raise the possibility that spontaneous folding of FimAa, which can insert either its N- or its C-terminal donor strand into its fold, is partially under kinetic control during the early stage of folding: The previously reported folding rates predict that about 50% of the FimAa molecules should initially fold to a structure equivalent to FimA wt and that the other 50% should fold to the FimAa conformation with antiparallel insertion of the C-terminal donor strand observed in the FimAa NMR structure. As the latter conformation is infinitely stable against unfolding ($k_{\text{unfolding}} = 1.8 \times 10^{-19} \text{ s}^{-1}$) and FimA wt unfolds about once per day [12], it might thus take several days until all molecules of FimAa reach the most stable conformation with antiparallel insertion of the C-terminal donor strand copy.

It was proposed that the physiological significance of soluble, folded FimA monomers could be that they represent a FimA storage form *in vivo* under conditions where FimA molecules are present at excess over the assembly chaperone FimC in the *E. coli* periplasm. Indeed, FimA wt can rebind to FimC after spontaneous

unfolding and refolding in the presence of FimC [12]. However, recent results suggest that FimA monomers could play a very important role in the infection mechanism of Gram-negative pathogens bearing type 1 pili. Notably, a soluble form of FimA from *E. coli*, *Salmonella* and *Shigella* culture supernatants proved to be a potent inhibitor of apoptosis of infected host epithelium cells, an innate host defense mechanism against propagation of internalized pathogens [21]. The structure of FimA wt monomers solved in this study readily provides the molecular basis of the existence of soluble forms of FimA. The differences in the modes of donor strand insertion between FimA wt and FimAa can be considered as a 180° rotation of the donor strand segment around His11 (Fig. 3a and c). This becomes possible by the presence of the two glycine residues (Gly8 and Gly14), three residues before and after His11, as the FimA pilin fold can only accept a glycine residue from the donor strand at the P4 side-chain pocket without steric disruption of the β -sheet main-chain hydrogen bonding network. The sequence of the natural FimA donor strand thus can be considered pseudo-palindromic. Among all other type 1 pilus subunits, this feature is only present in the donor strand of FimI (sequence ... G¹¹N¹²V¹³Q¹⁴F¹⁵Q¹⁶G¹⁷ ..., with Gln14 being equivalent to His11 in FimA), the subunit that has been proposed to terminate pilus assembly [35]. Most strikingly, however, the motif of the two glycines separated by five residues in the natural donor strand is preserved in the FimA pilus subunits of many other pathogenic enterobacteria (Fig. 3d). The intramolecular, parallel donor strand insertion observed for *E. coli* FimA wt may therefore be the common mechanism underlying the formation and occurrence of soluble FimA monomers in pathogens bearing adhesive pili. Many other pathogens may therefore produce FimA monomers as off-pathway products of pilus assembly to inhibit the apoptotic defense cascade of infected host cells and promote pathogen propagation.

Accession numbers

Coordinates have been deposited in the Protein Data Bank with accession number 2M5G; the resonance

Fig. 3. Details of parallel and antiparallel donor strand insertion into the FimA fold. (a) Superposition of the structures of the donor strands of FimAa (green) and FimA wt (red) in a cartoon representation. Side chains that occupy binding pockets (P0–P5) and three additional side chains are represented with sticks. Large side chains of phenylalanines and valines occupy the spacious pockets P0, P2, P3 and P5, while the shallow P1 and P4 positions accommodate glycines [34]. Val16 of FimA resides in a roomy expansion of the binding groove. (b) Superposition of the structures of free FimA (cyan and red) and the donor strand depleted variant FimA_t (blue) in complex with FimC; of FimC, only the β -strand complementing the FimA_t fold is shown (yellow). Topology and secondary structure elements are the same in both FimA molecules. The complementing β -strand of FimC (yellow) has the same orientation as the N-terminal donor strand in the structure of FimA wt. (c) Donor strands (with residue numbers) of FimA wt and FimAa aligned according to their interaction with the FimA pilin domain. Green arrows indicate the Gly residues accommodated by the P4 pocket. Residues that bind to the binding pockets in the structures of FimAa and FimA wt are indicated in red. (d) Sequence alignment of the N-terminal donor strand segment of FimA (and PapA) from other pilated enterobacteria, showing the conserved glycine pair (red), separated by five residues, allowing donor strand insertion in both orientations.

assignments are deposited in the Biological Magnetic Resonance Data Bank with accession code 15423.

Acknowledgements

We thank Dr. Pierre Barraud (ETH Zurich) for help with structure calculation. This project was supported by the Swiss National Science Foundation (SNF) and the ETH Zurich in the framework of the National Center of Competence in Research Structural Biology Program and SNF projects 138677 and 31003A-122095 to R.G.; G.W. acknowledges the SNF and ETH Zurich for financial support (SNF project 200021_120048 and ETH project 23 10-2).

Appendix A. Supplementary data

Supplementary data to this article can be found online at <http://dx.doi.org/10.1016/j.jmb.2013.10.029>.

Received 14 August 2013;

Received in revised form 4 October 2013;

Accepted 22 October 2013

Available online 30 October 2013

Keywords:

pili;
usher;
protein folding;
type 1 pili;
bacterial pathogenesis

Abbreviations used:

wt, wild type; SNF, Swiss National Science Foundation.

References

- [1] Zhou G, Mo WJ, Sebbel P, Min G, Neubert TA, Glockshuber R, et al. Uroplakin Ia is the urothelial receptor for uropathogenic *Escherichia coli*: evidence from *in vitro* FimH binding. *J Cell Sci* 2001;114:4095–103.
- [2] Hahn E, Wild P, Hermanns U, Sebbel P, Glockshuber R, Haner M, et al. Exploring the 3D molecular architecture of *Escherichia coli* type 1 pili. *J Mol Biol* 2002;323:845–57.
- [3] Waksman G, Hultgren SJ. Structural biology of the chaperone-usher pathway of pilus biogenesis. *Nat Rev Microbiol* 2009;7:765–74.
- [4] Sauer FG, Remaut H, Hultgren SJ, Waksman G. Fiber assembly by the chaperone-usher pathway. *Biochim Biophys Acta* 2004;1694:259–67.
- [5] Crespo MD, Puorger C, Schärer MA, Eidam O, Grutter MG, Capitani G, et al. Quality control of disulfide bond formation in pilus subunits by the chaperone FimC. *Nat Chem Biol* 2012;8:707–13.
- [6] Vetsch M, Puorger C, Spirig T, Grauschopf U, Weber-Ban EU, Glockshuber R. Pilus chaperones represent a new type of protein-folding catalyst. *Nature* 2004;431:329–33.
- [7] Nishiyama M, Ishikawa T, Rechsteiner H, Glockshuber R. Reconstitution of pilus assembly reveals a bacterial outer membrane catalyst. *Science* 2008;320:376–9.
- [8] Saulino ET, Thanassi DG, Pinkner JS, Hultgren SJ. Ramifications of kinetic partitioning on usher-mediated pilus biogenesis. *EMBO J* 1998;17:2177–85.
- [9] Phan G, Remaut H, Wang T, Allen WJ, Pirker KF, Lebedev A, et al. Crystal structure of the FimD usher bound to its cognate FimC-FimH substrate. *Nature* 2011;474:49–53.
- [10] Choudhury D, Thompson A, Stojanoff V, Langermann S, Pinkner J, Hultgren SJ, et al. X-ray structure of the FimC-FimH chaperone-adhesin complex from uropathogenic *Escherichia coli*. *Science* 1999;285:1061–6.
- [11] Valenski ML, Harris SL, Spears PA, Horton JR, Orndorff PE. The product of the *fimI* gene is necessary for *Escherichia coli* type 1 pilus biosynthesis. *J Bacteriol* 2003;185:5007–11.
- [12] Puorger C, Vetsch M, Wider G, Glockshuber R. Structure, folding and stability of FimA, the main structural subunit of type 1 pili from uropathogenic *Escherichia coli* strains. *J Mol Biol* 2011;412:520–35.
- [13] Puorger C, Eidam O, Capitani G, Erilov D, Grutter MG, Glockshuber R. Infinite kinetic stability against dissociation of supramolecular protein complexes through donor strand complementation. *Structure* 2008;16:631–42.
- [14] Vetsch M, Erilov D, Moliere N, Nishiyama M, Ignatov O, Glockshuber R. Mechanism of fibre assembly through the chaperone-usher pathway. *EMBO Rep* 2006;7:734–8.
- [15] Remaut H, Rose RJ, Hannan TJ, Hultgren SJ, Radford SE, Ashcroft AE, et al. Donor-strand exchange in chaperone-assisted pilus assembly proceeds through a concerted beta strand displacement mechanism. *Mol Cell* 2006;22:831–42.
- [16] Eshdat Y, Silverblatt FJ, Sharon N. Dissociation and reassembly of *Escherichia coli* type 1 pili. *J Bacteriol* 1981;148:308–14.
- [17] McMichael JC, Ou JT. Structure of common pili from *Escherichia coli*. *J Bacteriol* 1979;138:969–75.
- [18] Salit IE, Gotschlich EC. Type I *Escherichia coli* pili: characterization of binding to monkey kidney cells. *J Exp Med* 1977;146:1182–94.
- [19] Zavialov AV, Berglund J, Pudney AF, Fooks LJ, Ibrahim TM, MacIntyre S, et al. Structure and biogenesis of the capsular F1 antigen from *Yersinia pestis*: preserved folding energy drives fiber formation. *Cell* 2003;113:587–96.
- [20] Vetsch M, Sebbel P, Glockshuber R. Chaperone-independent folding of type 1 pilus domains. *J Mol Biol* 2002;322:827–40.
- [21] Sukumaran SK, Fu NY, Tin CB, Wan KF, Lee SS, Yu VC. A soluble form of the pilus protein FimA targets the VDAC-hexokinase complex at mitochondria to suppress host cell apoptosis. *Mol Cell* 2010;37:768–83.
- [22] DeLano WL, Lam JW. PyMOL: a communications tool for computational models. *Abstr Pap Am Chem Soc* 2005;230:U1371–2.
- [23] Wider G, Dreier L. Measuring protein concentrations by NMR spectroscopy. *J Am Chem Soc* 2006;128:2571–6.
- [24] Fairbrother WJ, Palmer AG, Skelton NJ. Protein NMR spectroscopy principles and practice. Elsevier Science; 1995.
- [25] Herrmann T, Güntert P, Wüthrich K. Protein NMR structure determination with automated NOE assignment using the

- new software CANDID and the torsion angle dynamics algorithm DYANA. *J Mol Biol* 2002;319:209–27.
- [26] Herrmann T, Güntert P, Wüthrich K. Protein NMR structure determination with automated NOE-identification in the NOESY spectra using the new software ATNOS. *J Biomol NMR* 2002;24:171–89.
- [27] Güntert P. Automated NMR structure calculation with CYANA. *Methods Mol Biol* 2004;278:353–78.
- [28] Brünger AT, Adams PD, Clore GM, DeLano WL, Gros P, Grosse-Kunstleve RW, et al. Crystallography & NMR system: a new software suite for macromolecular structure determination. *Acta Crystallogr Sect D Biol Crystallogr* 1998;54:905–21.
- [29] Laskowski RA, MacArthur MW, Moss DS, Thornton JM. PROCHECK: a program to check the stereochemical quality of protein structures. *J Appl Crystallogr* 1993;26:283–91.
- [30] Gossert AD, Bettendorff P, Puorger C, Vetsch M, Herrmann T, Glockshuber R, et al. NMR structure of the *Escherichia coli* type 1 pilus subunit FimF and its interactions with other pilus subunits. *J Mol Biol* 2008;375:752–63.
- [31] Eidam O, Dworkowski FSN, Glockshuber R, Grutter MG, Capitani G. Crystal structure of the ternary FimC-FimF(t)-FimD(N) complex indicates conserved pilus chaperone-subunit complex recognition by the usher FimD. *FEBS Lett* 2008;582:651–5.
- [32] Anderson KL, Billington J, Pettigrew D, Cota E, Simpson P, Roversi P, et al. An atomic resolution model for assembly, architecture, and function of the Dr adhesins. *Mol Cell* 2004;15:647–57.
- [33] Wüthrich K, Spitzfaden C, Memmert K, Widmer H, Wider G. Protein secondary structure determination by NMR: application with recombinant human cyclophilin. *FEBS Lett* 1991;285:237–47.
- [34] Sauer FG, Pinkner JS, Waksman G, Hultgren SJ. Chaperone priming of pilus subunits facilitates a topological transition that drives fiber formation. *Cell* 2002;111:543–51.
- [35] Rossolini GM, Muscas P, Chiesurin A, Satta G. Analysis of the *Salmonella* fim gene cluster: identification of a new gene (fimi) encoding a fimbrin-like protein and located downstream from the fima gene. *FEMS Microbiol Lett* 1993;114:259–65.